Luminescent Cr^{3+} centres in $KZnF_3$: an investigation of the vibronic effects

1990 J. Phys.: Condens. Matter 2 3997

(http://iopscience.iop.org/0953-8984/2/17/010)

J. Phys.: Condens. Matter 2 (1990) 3997–4003. Printed in the UK

Luminescent Cr^{3+} centres in $KZnF_3$: an investigation of the vibronic effects

Y Vaills†§, J Y Buzaré† and M Rousseau‡

† Laboratoire de Spectroscopie du Solide, UA 807, Faculté des Sciences, Route de Laval, 72017 Le Mans Cédex, France

‡ Laboratoire de Physique de l'Etat Condensé, UA 807, Faculté des Sciences, Route de Laval, 72017 Le Mans Cédex, France

Received 22 May 1989

Abstract. We present a detailed analysis of the emission band at 13 000 cm^{-1} in $KZnF_3:Cr^{3+}$. The spectrum structure at low temperature is interpreted in terms of zero-phonon lines and their replicas which are due to interaction with localised modes of both the defects and phonons of the host lattice.

1. Introduction

In the last few years, there has been a renewed interest in the so-called vibronic state lasers, due to their large range of frequency tunability and their potential high power. The laser materials are insulating fluoride or oxide single crystals doped with transition-metal ions. The tunable solid state lasting effect is connected with the interplay between the crystal field at the lasing ion and the electron–phonon coupling allowing broad-band absorption and emission. However, although many systems have been studied and operated successfully, there is sometimes a lack of spectroscopic data which prevents a full understanding of the lasing properties.

The laser ion Cr^{3+} has attracted much attention because of its excellent optical properties in ionic crystals even at room temperature. Most of the vibronic lasers such as alexandrite, emerald, garnet and tungstate lasers have been based on Cr^{3+} doped oxide crystals (Vivien 1986). Beside these systems, Cr^{3+} doped cubic $KZnF_3$ was first broadly tunable fluoride laser crystal to operate at room temperature (Brauch and Durr 1984) over several nanometres. The luminescence of Cr^{3+} ions in $KZnF_3$ at 13 000 cm^{-1} due to $^4A_2 \rightarrow {}^4T_2$ transition has been previously studied by Brauch (1983) and Pilla *et al* (1988).

In this paper we show how work initiated in our laboratory with the EPR study of $KZnF_3:Cr^{3+}$ (Binois *et al* 1973), extended later with the determination of the phonon dispersion curves of $KZnF_3$ (Rousseau *et al* 1981, Lehner *et al* 1982) and the application for the interpretation of the luminescence band of Ni^{++} in $KZnF_3$ (Russi *et al* 1984) leads us to improve the description of the vibronic interactions in $KZnF_3:Cr^{3+}$.

§ Present address: Laboratoire d'Etudes Physiques des Matériaux, UFR Faculté des Sciences, Université d'Orléans, 45067 Orléans Cédex 2, France

0953-8984/90/173997 + 07 $03.50

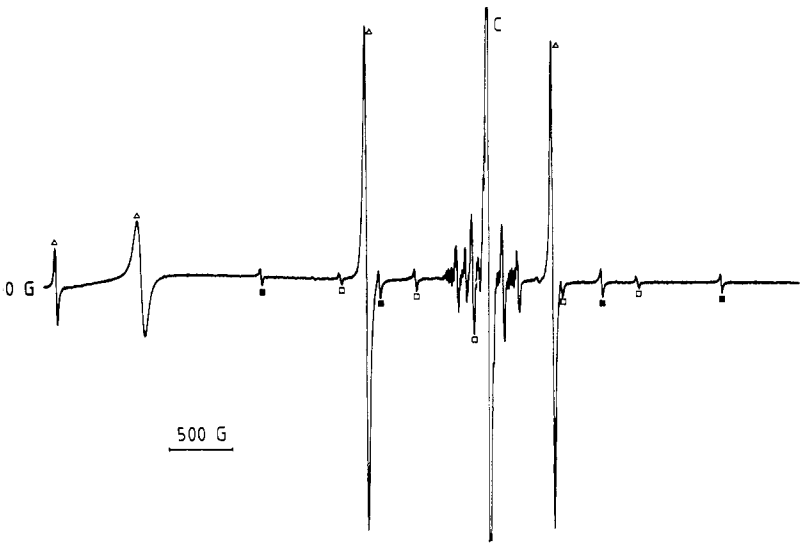

Figure 1. The $KZnF_3:Cr^{3+}$ EPR spectrum for $0\ G < H < 6000\ G$. $\nu \simeq 9.5$ GHz; $\boldsymbol{H}_0 \| \langle 100 \rangle$, $\boldsymbol{H}_{osc} \| \langle 110 \rangle$; C: cubic site; △: trigonal site; □: tetragonal site; ■: tetragonal site.

2. Experimental details

The $KZnF_3$ was synthesised, using the Bridgman–Stockbärger method in a platinum crucible moving through a vertical temperature gradient, from high purity powders of KF and ZnF_2. The sample was heavily doped with Cr_2O_3 ($\simeq 1\%$). The single crystal was of very good optical quality; it was green in colour and was free of visible inhomogeneities. Once produced, it was orientated using x-ray diffraction. We noticed that the small values of the atomic factors of the different ions contained in the crystal studied imposed very long exposure times for the Laue negatives. Finally a $0.4 \times 0.4 \times 0.6\ cm^3$ sample was sawed with a diamond saw and finely polished for the luminescence study.

The EPR spectra were recorded at room temperature on a Bruker X-band spectrometer ($\nu \simeq 9.5$ GHz). The static magnetic field may be varied from 0 to 10 000 G.

The luminescence study was done using a triple-monochromator DILOR Z 24 Raman spectrometer in the 90° scattering configuration with 400 μm slit width (resolution $<2\ cm^{-1}$). From $T = 300$ K to $T = 20$ K the sample was held in a variable-temperature cryogenerator, and for $T < 20$ K we have used a liquid helium cryostat.

3. EPR results

Trivalent chromium Cr^{3+} is substituted for divalent Zn^{2+} in the perovskite lattice $KZnF_3$. The EPR spectrum is shown in figure 1 when the magnetic field is directed along a ⟨001⟩ direction. Four site-characteristic lines are identified according to Binois *et al* (1973). The intense central line (C) is connected with Cr^{3+} ions in cubic sites (see figure 2). The □ and ■ lines are related to the tetragonal sites already mentioned by Binois; the △ lines arise from Cr^{3+} in the trigonal sites. The values of the spin Hamiltonian parameters are in agreement with those listed by Binois *et al* (1973). We recall that the □ defect had

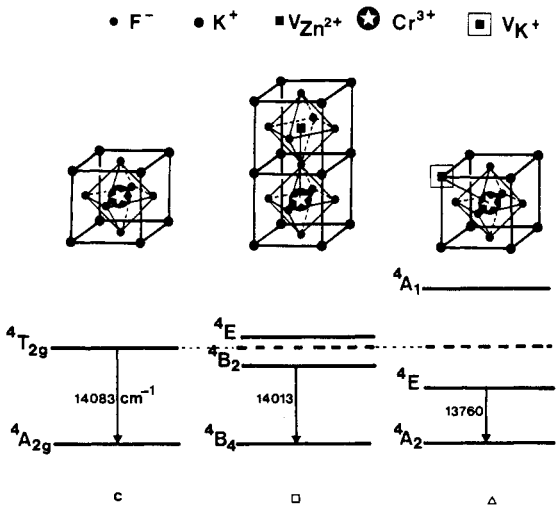

Figure 2. The energy levels of the Cr^{3+} sites in $KZnF_3$ (Brauch 1983) and their respective identification (Binois *et al* 1973).

been tentatively attributed to the pairing of a Cr^{3+} ion with a Zn^{2+} vacancy whereas the ■ defect had not been clearly interpreted. The trigonal defect is due to the pairing of a Cr^{3+} ion with a K^+ vacancy at a nearest-neighbour site. The only difference between this and Binois' work (Binois *et al* 1973, Binois 1974) is the relative intensity of the trigonal lines which is larger in our sample. Furthermore, Brauch mentions the C, □ and △ lines only.

4. Luminescence results

At room temperature the $KZnF_3:Cr^{3+}$ emission spectrum is characterised by a 1500 cm^{-1} linewidth Gaussian band centred around 13 000 cm^{-1}.

As the temperature is decreased from room temperature to $T = 10$ K, sharp lines and their vibronic replicas appear superimposed on the broad band. The spectra recorded at various temperatures using the 514.5 nm line as a pump line are shown in figure 3. Some spectra were also recorded using $\lambda = 457.9$ nm (figure 4) and $\lambda = 476.5$ nm as pump lines.

The independence of the absolute positions of the observed lines of the excitation wavelength proves beyond doubt that the phenomenon is luminescence. We notice that the intensities of the sharp lines decrease rapidly when the temperature increases. However, the large band intensity decreases with temperature.

5. Discussion

At low temperature the spectrum presents many interesting peculiarities which are not easily interpretable. Referring to the energy level scheme proposed by Brauch (1983) and recalled in figure 2, at 10 K three zero-phonon lines corresponding to the three Cr^{3+} sites shown in figure 2 are identified as follows:

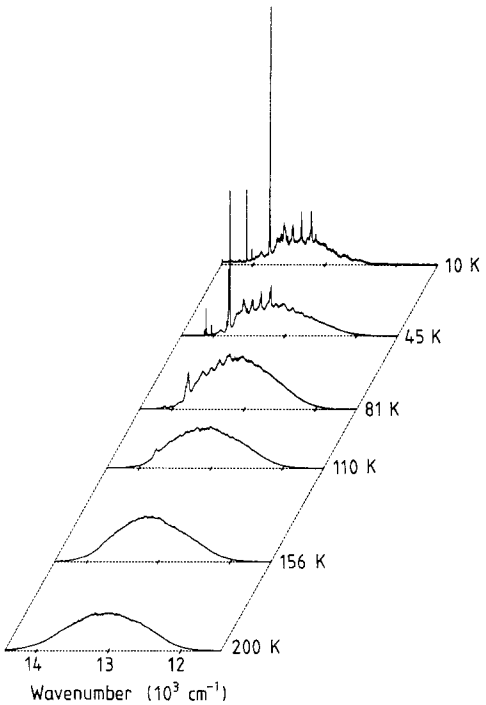

Figure 3. The temperature dependence of the $KZnF_3:Cr^{3+}$ luminescence spectra.

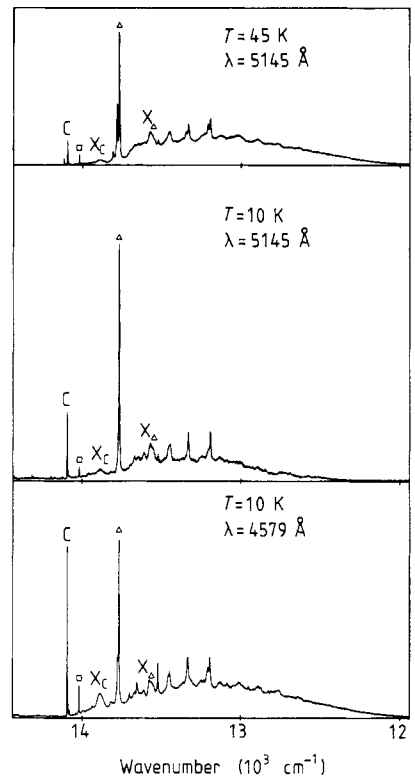

Figure 4. The temperature and excitation wavelength effects on the $KZnF_3:Cr^{3+}$ luminescence spectra.

(i) C lines: $\sigma = 14\,091$† cm^{-1} ($14\,083$‡ cm^{-1}): cubic site $^4T_{2g} \rightarrow {}^4A_{2g}$ transition;
(ii) △ lines: $\sigma = 13\,765$† cm^{-1} ($13\,760$‡ cm^{-1}): trigonal site $^4E \rightarrow {}^4A_2$ transition;
(iii) □ lines: $\sigma = 14\,016$† cm^{-1} ($14\,013$‡ cm^{-1}): tetragonal site $^4B_2 \rightarrow {}^4B_1$ transition.

Nevertheless Pilla *et al* (1988) mention that the assignment of □ to tetragonal centres is not unequivocal because its lifetime coincides with that of the cubic one. Furthermore its luminescence intensity relative to C and △ is different from the relative concentration of tetragonal centres as deduced from EPR. This last point should be treated with some caution because the relative intensity of the zero-phonon lines is strongly affected by the wavelength of the laser excitation. In fact, as seen in figure 4, the C line associated with the highest energy transition is much more intense with $\lambda = 4579$ Å used as a pump line than with $\lambda = 4765$ Å or 5145 Å.

In order to obtain a deeper insight into the various contributions to the luminescence spectrum, we have tried to reconstruct the lowest temperature emission band by considering the multiphonon replicas of the zero-phonon lines with the continuous distribution of modes given by the phonon density of states. As previously, in calculating the emission band at 20 000 cm^{-1} in $KZnF_3:Ni$, we have worked with Pryce's model

† Our results.
‡ Brauch's results.

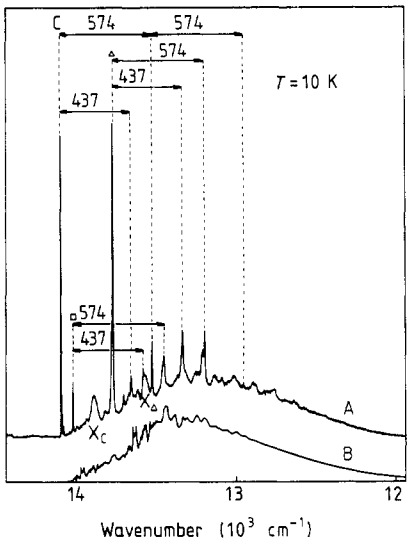

Figure 5. The $KZnF_3:Cr^{3+}$ luminescence spectrum. A: experimental spectrum ($\lambda = 4579$ Å); B: calculated multiphonon contribution.

(Pryce 1966) assuming a linear coupling between the electronic state and the crystal vibrations. In a first approach we have taken the same coupling constant S to represent the modulation of the three electronic states (cubic–tetragonal–trigonal) by the crystal vibration modes of the overall Brillouin zone.

In Pryce's notation, the continuous emitted spectrum is approximated by

$$I(h\nu) = \frac{64\pi^4\nu^4}{3c^3} \sum_{p=1}^{\infty} e^{-S} \frac{S^p}{p!} B_p(h\nu)$$

where $B_p(h\nu)$, defined from the normalised phonon density of states (Russi *et al* 1984), represents the p phonon contribution.

In the framework of this model, the broad emission band is well simulated with a coupling constant $S = 3.7 \pm 0.2$. This value is very close to $S = 3.8$ previously given for $KZnF_3:Ni^2$ (Russi *et al* 1984) and $S \simeq 4$ estimated by Kunzel *et al* (1981) for $KZnF_3:Co^{2+}$. The comparison between the experimental emission band and the calculated one, both represented on figure 5, clearly shows that the sharp lines not attributed to zero-phonon lines cannot be interpreted in terms of vibronic interactions with the phonons of the host lattice. In fact, most of these lines are shifted from the zero-phonon lines by multiples of 437 cm^{-1} or 574 cm^{-1}. When looking at the phonon density of states determined by Rousseau *et al* (1981) it is clear that 437 cm^{-1} lies in the vicinity of a gap in the phonon density of states whereas 574 cm^{-1} is greater than the upper cut-off frequency of this material. Thus the lines may be reasonably attributed to replicas of the purely electronic lines due to interactions with localised vibrations at 437 cm^{-1} and 574 cm^{-1}. The identification of these replicas has been guided and made easier by considering the trigonal lines ($\triangle$ on figure 4) which can be easily recognised because of the two following features:

(i) their low temperature intensities are always strong whatever the wavelength of the excitation line;

(ii) their complicated shapes (commented on below) permit us to recognise them unambiguously.

On the other hand, these two frequencies (574 cm^{-1} and 437 cm^{-1}) correspond to the usual frequencies for normal vibrations of $M^{III}F_6$ octahedra in $AAlF_4$ compounds (Bulou 1985). Furthermore, two symmetric A_{1g} vibration modes involving Cr^{3+} and F^- ions have been reported at 586 cm^{-1} and 466 cm^{-1} in Rb_2CrF_5 (Boulard *et al* 1989). From the evaluation of the relative intensity ratio of the different lines corresponding to successive replicas of the same zero-phonon line, the Huang–Rhys factor characterising the electron coupling with the two localised modes was estimated to be $S \simeq 0.16$.

In the framework of our description, the main features of the emission spectrum are interpreted with the exception of the two broad lines denoted as X_c and $X_\triangle$ on figure 5. As shown on figure 4, the intensities of these two lines are related to the relative intensities of the cubic and trigonal zero-phonon lines respectively and they both lie at 200 cm^{-1} from these zero-phonon lines. In fact, this frequency shift corresponds exactly to the frequency of the Brillouin zone centre transverse optical mode having the largest oscillator strength (Ridou *et al* 1986). Then, a strong coupling between the electronic states and all the phonon modes having similar normal coordinates can produce a broad line in the luminescence spectrum even without any significant singularity in the phonon density of states.

Finally, some particular features of the spectra have to be outlined even if it is not possible to draw definite conclusions about them. At 45 K (see figure 4), the trigonal line, marked $\triangle$, is flanked by a less intense line $\triangle'$. Their vibronic replicas at 437 and 574 cm^{-1} are clearly apparent and so confirm the idea of localised modes. The splitting between $\triangle$ and $\triangle'$ is equal to 15 cm^{-1} which is a typical spin–orbit coupling order of magnitude. As temperature decreases, the $\triangle'$ line intensity decreases whatever the pump line is. Moreover a third component $\triangle''$ is present between $\triangle$ and $\triangle'$ with $\lambda =$ 4579 Å.

Finally, the line at 14 111 cm^{-1} may be tentatively attributed to a transition between ^4E and $^4B_4$ levels for a tetragonal site. However, the ratio

$$\Delta E(^4B_4 \rightarrow {}^4B_2) - \Delta E(^4A_{2g} \rightarrow {}^4T_{2g})/[\Delta E(^4B_4 \rightarrow {}^4E) - \Delta E(^4A_{2g} \rightarrow {}^4T_{2g})]$$

is not equal to 2 as it should be (its value is close to 4). It may be noticed that this line disappears at 10 K.

6. Conclusion

The present work points out that a good knowledge of the overall phonon dispersion curves of the host lattice can give useful information for the interpretation of the luminescence spectra of an isolated impurity in a crystal. In order to go further it is necessary to develop an analytic expression for the vibronic coupling coefficient for each normal mode as a function of its corresponding eigenvector. Some features of the spectra such as the splitting of the trigonal line and the influence of the wavelength excitation are not yet understood; in order to solve this problem, experiments with higher resolution and different pump lines are in progress.

References

Binois M 1974 *Thèse de 3ème Cycle* Paris
Binois M, Leblé A, Rousseau J J and Fayet J C 1973 *J. Physique Coll.* **34** C9 285

Boulard B, Rousseau M and Jacoboni C 1989 *J. Solid State Chem.* **80** 17–31
Brauch U 1983 *PhD Thesis* University of Stuttgart
Brauch U and Durr U 1984 *Opt. Commun.* **49** 61
Bulou A 1985 *Thèse d'Etat* Université P et M Curie
Kunzel W, Knierjm W and Burr U 1981 *Opt. Commun.* **36** 383
Lehner N, Rauh H, Strobel K, Geick R, Heger G, Bouillot J, Renker R, Rousseau M and Stirling W G 1982 *J. Phys. C: Solid State Phys.* **15** 6545
Pilla O, Galvanetto E, Montagna M and Vilian G 1988 *Phys. Rev.* B **38** 3477
Pryce M H L 1966 *Phonon in Perfect Lattices and in Lattices with Point Imperfections* ed R W H Stevenson (Edinburgh: Oliver and Boyd) p 403
Ridou C, Rousseau M and Gervais F 1986 *J. Phys. C: Solid State Phys.* **19** 5757–67
Rousseau M, Gesland J Y, Hennion B, Heger G and Renker B 1981 *Solid State Commun.* **38** 45
Russi R, Barbosa G A, Rousseau M and Gesland J Y 1984 *J. Physique* **45** 1773
Vivien D 1986 *Revue Phys. Appl.* **21** 709